

***Brucea javanica* Increases Survival and Enhances Gemcitabine Efficacy in a Patient-derived Orthotopic Xenograft (PDOX) Mouse Model of Pancreatic Cancer**

HAITAO YANG¹⁻³, ZHONG TONG¹⁻³, LEI SHEN⁴, YU SUN^{5,6}, ROBERT M. HOFFMAN^{5,6} and JUN HUANG¹⁻³

¹The Third Affiliated Hospital of Anhui Medical University, Hefei, P.R. China;

²Hefei First People's Hospital, Hefei, P.R. China;

³Hefei Binhu Hospital, Hefei, P.R. China;

⁴Hefei Third People's Hospital, Hefei, P.R. China;

⁵AntiCancer Inc., San Diego, CA, U.S.A.;

⁶Department of Surgery, UCSD, San Diego, CA, U.S.A.

Abstract. *Background/Aim:* Traditional Chinese medicine (TCM) *Brucea javanica* (BJO) has shown anti-proliferation efficacy on human carcinoma cells *in vitro*. The aim of the present study was to evaluate for the first time the efficacy of BJO combined with the first-line chemotherapeutic drug gemcitabine (GEM) on tumor growth-inhibition and survival in a pancreatic cancer patient-derived orthotopic xenograft (PDOX) mouse model. *Materials and Methods:* The pancreatic cancer tumor fragment originated from a patient at the Hefei First People's Hospital (Anhui, PR China). The surgical specimen was transplanted orthotopically in nude mice using surgical orthotopic implantation (SOI). All mice were randomized and assigned to 5 groups: G1: saline vehicle (0.1ml per mouse, oral, once per day); G2: GEM [100 mg/kg, intraperitoneal (i.p), twice per week]; G3: GEM+BJO [100 mg/kg GEM, i.p, twice per week+1g/kg BJO, oral, once per day (qd)]; G4: BJO (1g/kg, oral, qd). Group 5 and Group 6 were used to observe survival [G5: saline vehicle (0.1ml per mouse, oral, qd), G6: BJO (1g/kg, oral, qd)]. Body weight and tumor volume were measured twice per week. TUNEL staining was used to determine apoptosis. *Results:* The combination of GEM + BJO resulted in a reduced tumor growth rate ($p<0.05$) and greater apoptosis ($p<0.05$) compared to the vehicle control and GEM monotherapy. In addition, the BJO-treated group showed a statistically significant increase in survival compared to the vehicle control ($p<0.05$).

Correspondence to: Jun Huang, The Third Affiliated Hospital of Anhui Medical University & Hefei First People's Hospital & Hefei Binhu Hospital, Hefei, Anhui, 230061, P.R. China. Tel: +86 13966740069, e-mail: hj17161@163.com

Key Words: Pancreatic cancer, *Brucea javanica*, gemcitabine, PDOX, combination therapy, synergistic effect, survival.

Conclusion: BJO is a promising non-toxic TCM to effectively treat pancreatic cancer, both as monotherapy and in combination with first-line GEM therapy.

Pancreatic cancer has the lowest 5-year relative survival rate (6%) among all the malignant cancers in the United States due to resistance to first-line therapy, including gemcitabine (GEM) (1). In China, traditional Chinese medicine (TCM) has been used as an important adjuvant to cancer treatment (2).

Brucea javanica is an evergreen shrub that is widely distributed from southeast Asia to northern Australia (3). *Brucea javanica* oil (BJO) has been used *in vitro* against cell lines from gastrointestinal cancer (4-6), encephalophyma, lung cancer and lung cancer brain metastasis (7). Moreover, it has been reported that *Brucea javanica* fruit induces cytotoxicity and apoptosis in pancreatic adenocarcinoma cell lines *in vitro* (8), however its role *in vivo* has not been studied. In this regard, a pancreatic patient-derived orthotopic xenograft (PDOX) nude mouse model (9-15) was established for *in vivo* anti-tumor evaluation of BJO in the present study.

Materials and Methods

Patient-derived tumor collection. The tumor specimen originated from a 74-year-old woman with advanced pancreatic adenocarcinoma and diagnosed as pT4N0M0 stage, according to the AJCC cancer staging manual (16). Informed written consent was obtained under the IRB of Hefei First People's Hospital (Anhui, PR China), where surgery was performed (Figure 1A). Fresh samples were obtained from surgery and placed in RPMI 1640 (C11875500BT, Gibco, USA) culture medium for subsequent transplantation to the laboratory at the Anhui Medical University (Anhui, PR China) (17).

Animal care. Athymic female nude (*nu/nu*) mice, 4-5 week of age, 18-23g, were used in this study. All mice were obtained from Cavens Inc. (Changzhou, PR China). All mice were maintained in

a HEPA-filtered environment throughout the experiment, at a constant temperature of 24-25°C and humidity of 50-60%. All mice were fed with laboratory rodent diet. Cages, food and bedding were autoclaved.

Preparation of tumor stock. Mice were anesthetized by intramuscular injection of 0.02 ml of a solution of 50% ketamine, 38% xylazine, and 12% acepromazine maleate (18). The fresh tumor specimen in RPMI 1640 medium was cut into small pieces (3-5mm in diameter) and immediately transplanted to nude mice subcutaneously (*s.c.*). The subcutaneously-growing tumor stock was harvested and inspected when the volume reached 500 mm³ (10 mm in diameter); any suspected or grossly-necrotic tissue was removed. Healthy tumor tissues were subsequently cut into small fragments of approximately 1 mm³ and used for surgical orthotopic implantation (SOI) (19).

Test agents. Gemcitabine (GEM) was purchased from Hansho Pharmaceutical (Lianyungang, Jiangsu, PR China, Lot #619191013). *Brucea javanica oil* (BJO) capsule was purchased from Vanguard Pharmaceutical (Haimen, Jiangsu, PR China, Lot #1901061).

Establishment of PDOX nude mouse model. The pancreatic tumor fragments, harvested from the stock tumors, were transplanted by surgical orthotopic implantation (SOI) in nude mice. All surgical procedures were performed under an 8× magnification microscope using a HEPA-filtered laminar flow hood. Animals were anesthetized (18) and the surgical area was sterilized using iodine and alcohol. An incision of approximately 1 cm long was made in the left upper abdomen of each nude mouse using surgical scissors. The tail of the pancreas was exposed through this incision (20), the capsule at the transplantation site was stripped, and two tumor fragments (1 mm³) were transplanted and secured with 8-0 surgical sutures (nylon). The abdomen was closed with 6-0 surgical sutures (21). The schematic procedure for PDOX establishment is illustrated in Figure 2.

Treatment study design. Treatment was initiated 19 days after surgical orthotopic implantation (SOI). PDOX mice bearing tumors (n=30) were randomized and assigned to 6 groups of 5 mice based on tumor size: Group 1-Group 4 were used to evaluate tumor growth inhibition. G1: saline vehicle (0.1ml per mouse, oral, once per day); G2: GEM (100 mg/kg, intraperitoneal, twice per week); G3: GEM+BJO (100 mg/kg, *i.p.*, twice per week+1g/kg, oral, once per day); G4: BJO (1g/kg, oral, once per day). Group 5 and Group 6 were used to observe survival. G5: saline vehicle (0.1 ml per mouse, oral, once per day); G6: BJO (1 g/kg, oral, once per day). Body weight of the PDOX mice was weighted twice per week using an electronic scale. In G1-G4, an exploratory laparotomy was performed every 10 days to monitor primary tumor growth. Tumor volume was measured using a vernier caliper and estimated by measuring the perpendicular minor dimension (W) and major dimension (L). Approximate tumor volume was calculated with the formula $(W^2 \times L) / 2$. Data are presented as mean±standard deviation (SD) (22). All animals were euthanized 30 days after initial treatment. At autopsy, the abdomen was opened and the primary tumor was removed and weighed. The tumor growth inhibition (TGI) value in each group was calculated with the formula: $TGI (\%) = (1 - \text{mean tumor weight of the treated group} / \text{mean tumor weight of the control group}) \times 100\%$. In G5 and G6, the animals were

observed for survival and the date of death or euthanasia was recorded (23). A survival curve was drawn based on the date of death for survival evaluation.

Histopathological analysis. Hematoxylin and eosin (H&E) staining was performed on fresh tumor specimens collected from the patient during surgery and tumor tissue obtained from PDOX mice. Fresh tissue samples were fixed in 10% formalin and embedded in paraffin before sectioning and staining. Tissue sections (4 μm) were deparaffinized in xylene and rehydrated in an ethanol series. Finally, the sections were counterstained with hematoxylin and examined and images captured using a microscope (BX53F, Olympus Corp., Tokyo, Japan) equipped with a Q-IMAGE CCD digital camera (Teledyne Photometrics, Tucson, Arizona, US) (18).

Cell death detection (TUNEL). TUNEL staining was performed to determine apoptosis in each group, according to the manufacturer's instructions. The sections were deparaffinized with xylene and rehydrated using gradient ethanol. The permeable solution was then added for incubation at 37°C for 8 min. After rinsing with PBS, mixed TdT (50 μl) + dUTP (450 μl) were added to the treatment group, dUTP (50 μl) was added to the negative control group, 100 μl DNase I was added to the positive control group and then incubated at 25°C for 10 min. The slides were then rinsed with PBS. The converter-POD (50 μl) was added and incubated at 37°C for 30 min. After washing with PBS, the IDAB substrate (100 μl) was applied on the slides and reacted at 25°C for 10 min. The slides were then rinsed with PBS. Hematoxylin was added as a counter stain and sealed with neutral gum. The slides were observed using an optical microscope and the representative images were captured with a digital camera. The apoptosis index (AI) was analyzed using image Pro 6.0 software (Media Cybernetics, Silver Springs, MD, USA).

Statistical analysis. All data are represented as mean±standard deviation (SD). Statistical analysis was performed using GraphPad Prism 8.0 software (GraphPad Software, Inc. La Jolla, CA, USA). The analysis of one-way variance (ANOVA) followed by Bonferroni correction was used to compare mean tumor volume, tumor weight and body weight among the experimental groups. The Log-rank (Mantel-Cox) test was used to compare survival among the experimental groups. Data from animals that died or were sacrificed prior to the completion of the study were included in analyses up to the time of death. A *p*-value less than 0.05 was considered statistically significant.

Results

Establishment of the pancreatic PDOX mouse model. Tumor growth was monitored after the fresh patient-derived specimen was transplanted to 5 nude mice subcutaneously. Four of them had tumor growth. Forty-two days after transplantation, the mean tumor volume reached over 523.4 mm³ (Figure 3A). A tumor growth curve was then plotted (Figure 3B).

Forty nude mice were used for pancreatic PDOX implantation, 27 mice were found to develop tumors (67.5%).

Histopathological analysis. H&E staining was performed on both the original patient sample and PDOX tumor to confirm

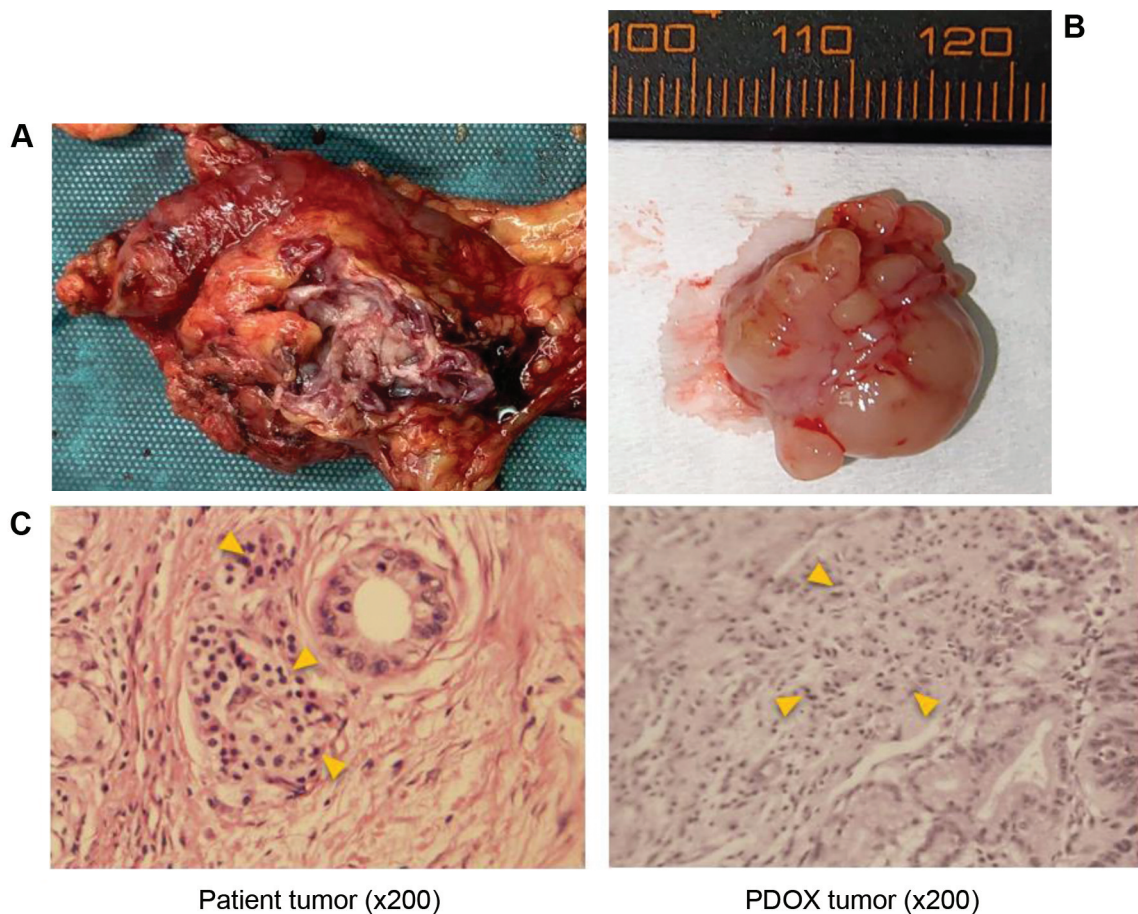


Figure 1. Histopathologic comparison of the PDOX tumor with the fresh patient tumor. (A) Fresh patient tumor obtained from surgery. (B) PDOX specimen of the vehicle control group. (C) Comparison of fresh patient tumor and xenograft tumor using H&E staining. The arrows show the abnormally abundant eosinophils (100× magnification).

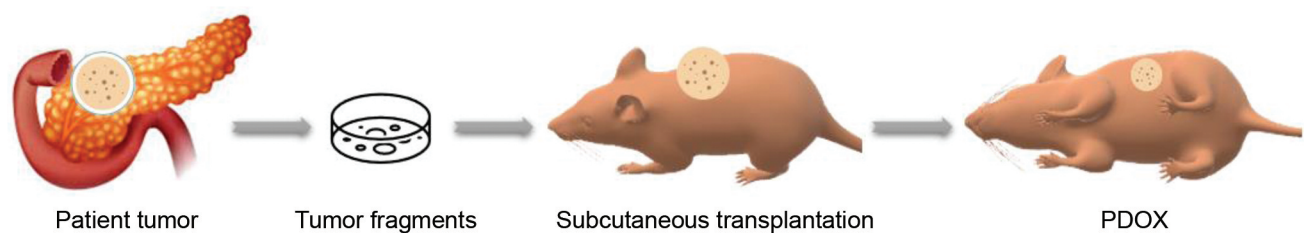


Figure 2. Schematic representation of the establishment of patient-derived orthotopic xenograft (PDOX) of pancreatic cancer.

the replication of the histopathologic characteristics in the PDOX model (Figure 1A, Figure 1B) (24). PDOX tumor sections showed that the glands were compromised of ductal structures with different degrees of differentiation, accompanied by abundant fibrous stroma and abundant eosinophilic cytoplasm. The pathological morphology was

consistent with the clinicopathological diagnosis of moderately differentiated ductal adenocarcinoma in the original tumor (Figure 1C).

Combination of GEM with BJO inhibits primary tumors. Treatment was initiated when the orthotopic tumors were

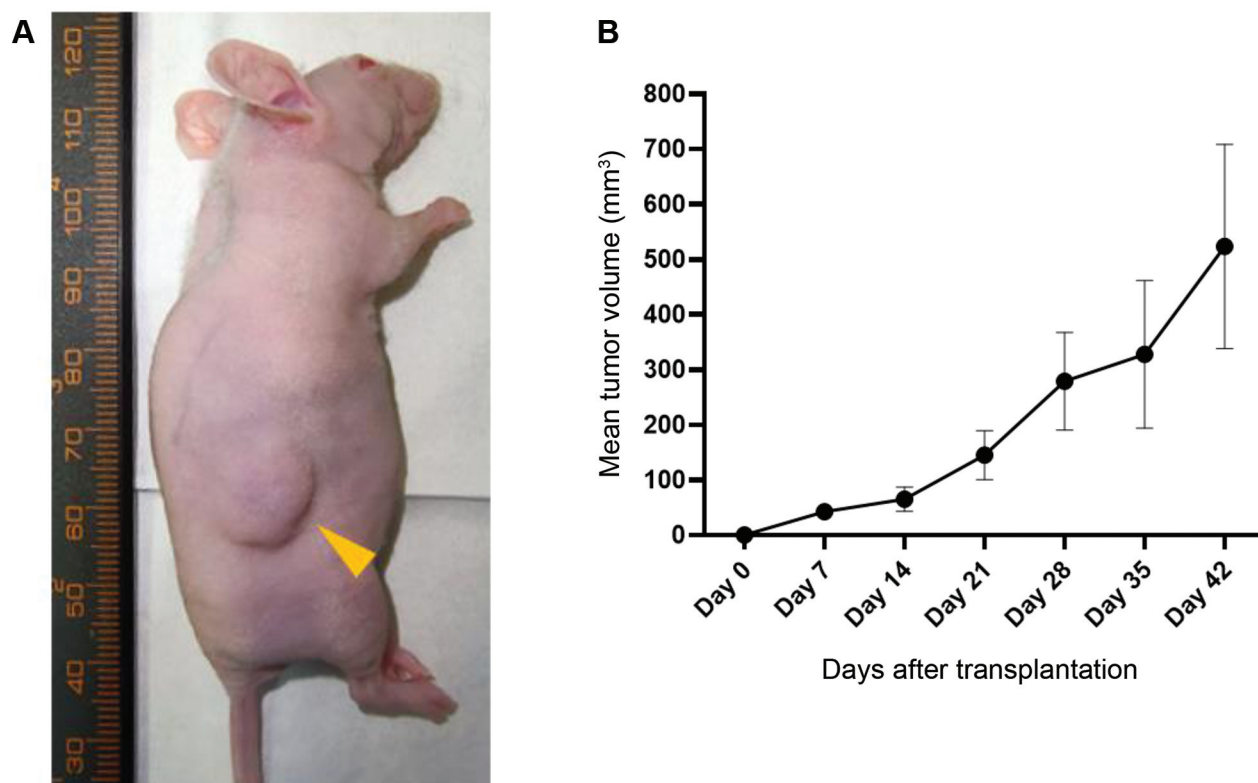


Figure 3. Establishment of the patient-derived subcutaneous tumor mouse. (A) The yellow arrow shows the patient-derived tumor grown subcutaneously in the nude mouse. (B) Growth curve of the subcutaneous tumor in nude mice.

approximately 100 mm³ (5-6 mm in diameter). Primary tumor volume was measured on day 1, 10, 20, 30, 40 by exploratory laparotomy after initial treatment. A tumor growth curve was plotted (Figure 4C). As shown in Figure 4A and Figure 4B, both Groups 2 (GEM) and 3 (GEM + BJO) demonstrated a statistically significant smaller tumor volume compared to the vehicle control during the entire treatment period ($p < 0.05$). Moreover, Group 3 (GEM + BJO) had greater inhibition efficacy and showed a statistically significant difference compared to Group 2 (GEM) ($p = 0.035$). Group 2 (GEM) and Group 3 (GEM + BJO) showed a statistically significant lower tumor weight compared to the vehicle control group ($p < 0.05$). GEM combined with BJO had a statistically-significant tumor inhibition compared to GEM alone ($p = 0.0059$) (Figure 4D). There was no difference between Group 1 (Vehicle) and Group 4 (BJO) for either tumor volume or tumor weight. The tumor growth inhibition (TGI) values are listed in Table I.

BJO prolongs survival in the pancreatic cancer PDOX mouse model. Treatment of BJO (G6) in the PDOX mice showed a statistically significant increase in survival compared to the saline vehicle control (G5) ($p = 0.0374$)

Table I. Efficacy of treatment on tumor weight in the pancreatic cancer-PDOX mouse model. The statistical-analysis was performed by one-way ANOVA. A p -Value < 0.05 is considered to be statistically significant.

Group	Tumor weight (g) Mean±SD	T/C (%)*	p -Value
G1 Vehicle	2.70±0.60	-	G1vsG2: 0.0272
G2 GEM	1.68±0.33	37.82%	G1vsG3: 0.0079
G3 GEM+BJO	1.08±0.43	60.10%	G1vsG4: 0.9999
G4 BJO	2.49±0.45	7.92%	G2vsG3: 0.0059

*TGI (%) = $(1 - \text{mean tumor weight of the treated group} / \text{mean tumor weight of the control group}) \times 100\%$.

(Figure 5). The medium survival days in Group 4 and Group 5 was 81 and 95 days, respectively.

BJO reduces GEM side-effects and improves general conditions in PDOX mice. Combination of BJO and GEM showed significantly lower body-weight loss rate than GEM monotherapy during the whole treatment period ($p < 0.05$) (Figure 6A, Figure 6B). BJO treated groups showed better

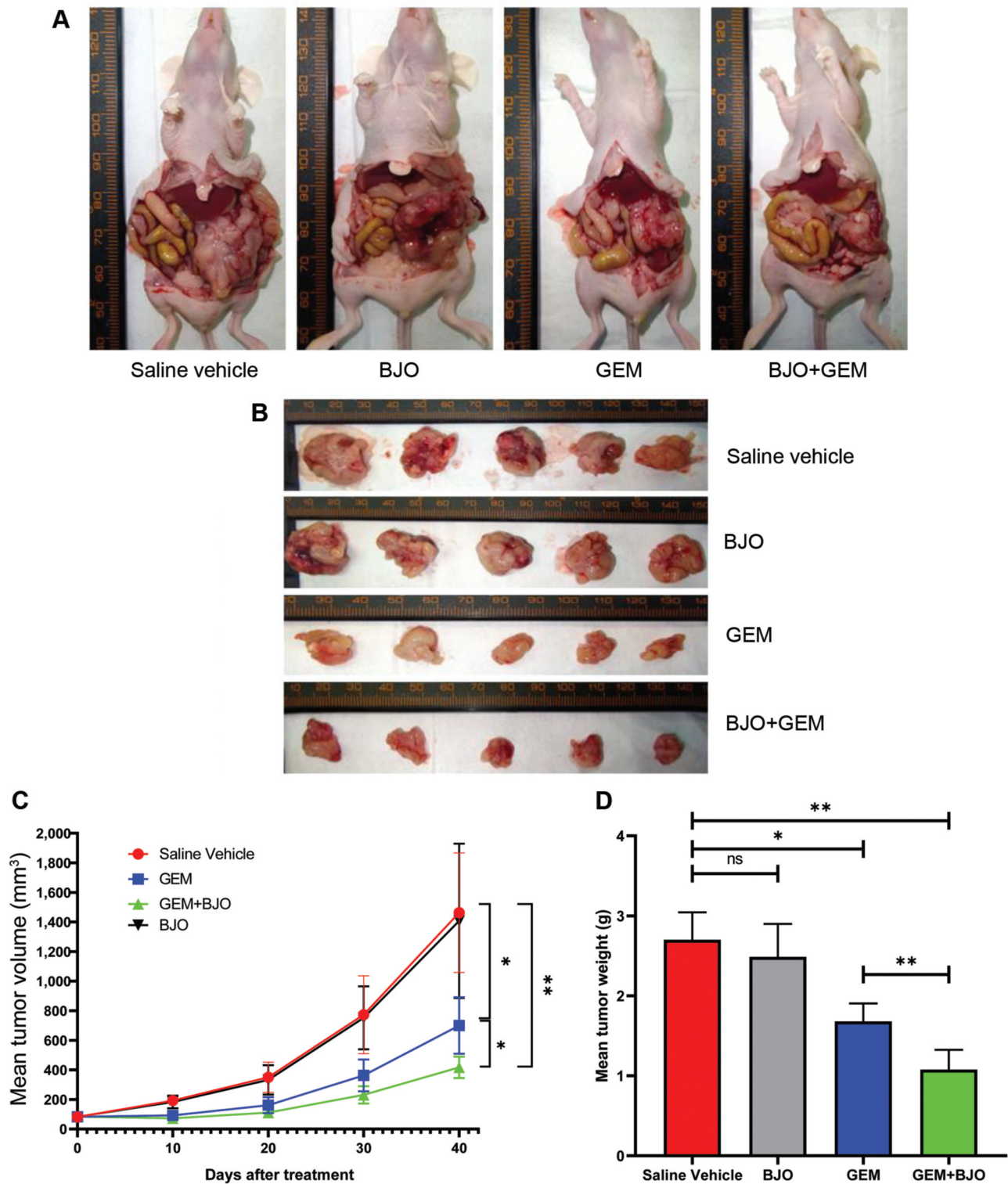


Figure 4. *Brucea javanica* oil (BJO) can synergistically enhance the inhibition of gemcitabine (GEM) on tumor growth. (A) Images of orthotopic xenograft tumors in each efficacy evaluation group at autopsy. (B) Images of excised primary tumor in each efficacy evaluation group at autopsy. (C) Tumor growth curve after treatment. * $p < 0.05$ (BJO+GEM compared to GEM alone), ** $p < 0.05$ (GEM compared to vehicle), *** $p < 0.01$ (BJO+GEM compared to vehicle). (D) Mean tumor weight in each efficacy evaluation group at the end of treatment. Data are represented as Mean \pm SD (n=5). * $p < 0.05$ (GEM compared to Vehicle), ** $p < 0.01$ (GEM+BJO compared to Vehicle, GEM+BJO compared to GEM). All data was analyzed using one-way ANOVA followed by Bonferroni correction.

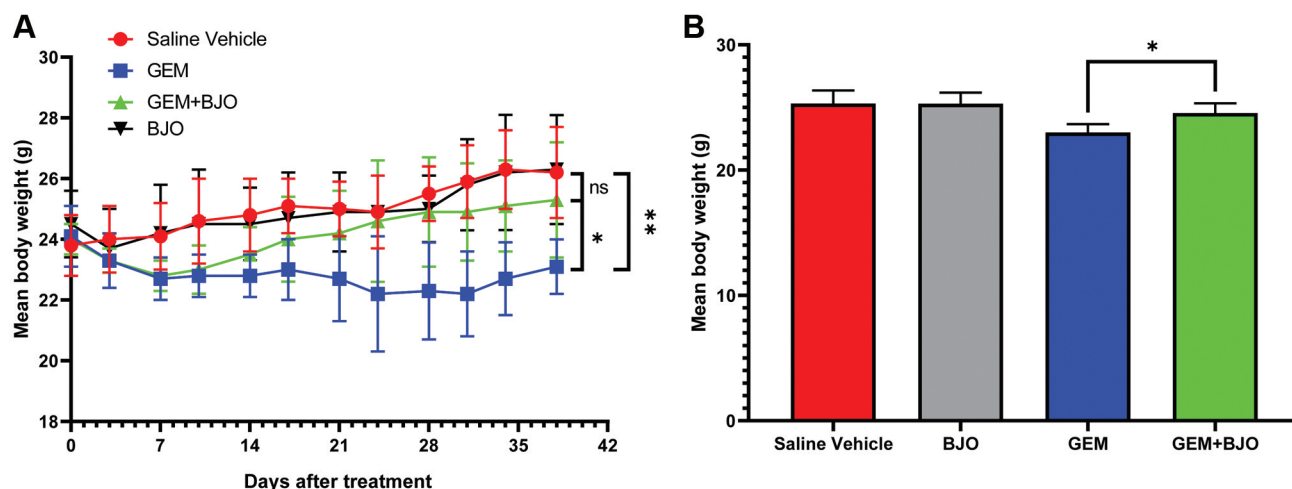


Figure 5. Effect of *Brucea javanica* oil (BJO) and gemcitabine (GEM) on body weight in the PPC-PDOX mouse model. GEM combined with BJO could reduce body weight compared to GEM treatment alone. (A) Body weight observing curve in each group containing each measurement point. * $p < 0.05$ (GEM compared to GEM+BJO), ** $p < 0.01$ (GEM compared to Vehicle). (B) Medium body weight in each group during treatment. * $p < 0.05$ (GEM compared to GEM+BJO). All data was analyzed using one-way ANOVA followed by Bonferroni correction.

activity and smoother skin during the treatment period indicating that BJO could improve the general condition in pancreatic cancer PDOX mice.

BJO synergistically enhances the apoptotic effect of GEM in vivo. The result of TUNEL staining demonstrated that BJO treated alone did not significantly induce apoptosis compared to the saline vehicle ($p > 0.05$). However, in combination with GEM, it showed significantly higher apoptosis than GEM monotherapy ($p = 0.044$) (Figure 7A, Figure 7B).

Discussion

Brucea javanica was first recorded as a TCM approximately 250 years ago in Chinese medical books (25). It has been reported to have many biological properties including anti-malarial, anti-leukemic, antiviral, anti-inflammatory and antitumor (5, 26-28). In China, it has been used as an adjuvant treatment for lung, liver and stomach cancer in the clinic (6, 29, 30). It was reported that BJO can induce apoptosis in a variety of cancers including pancreatic cancer (4, 8, 25, 31-33). However, most of the studies were performed on cell lines *in vitro*. In the present study, for the first time the efficacy of BJO was evaluated *in vivo* using a pancreatic cancer PDOX mouse model. Compared to the traditional orthotopic xenograft mouse model, PDOX models are established with fresh histologically intact human tumor tissues that closely resemble the human patient and can facilitate optimal individual therapy (34).

We designed two parallel trials, one to evaluate tumor-growth inhibition and the other to monitor survival. In the

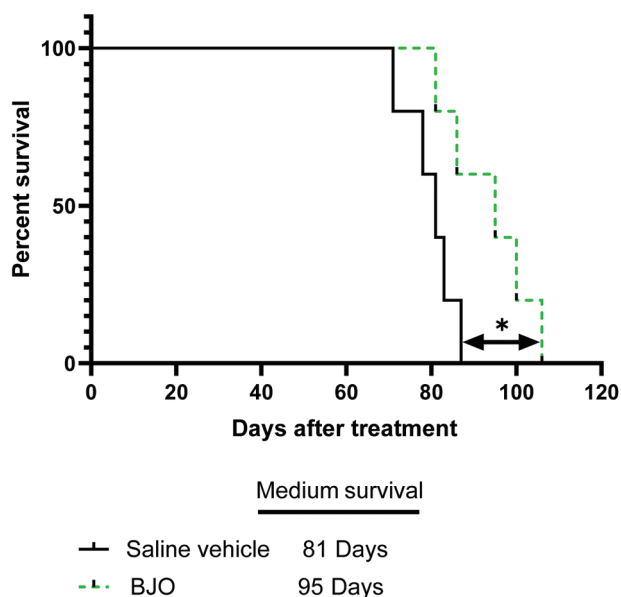


Figure 6. Log-rank survival analysis of mice treated with *Brucea Javanica* oil (BJO) versus saline, using the pancreatic cancer-PDOX mouse model. The medium survival was 81 days for the Vehicle group versus 95 days for the BJO group. * $p < 0.05$ (compared to vehicle).

efficacy evaluation groups, we found that the group treated with BJO alone had limited tumor-growth inhibition. When BJO was combined with GEM, it could significantly decrease tumor growth compared to GEM alone. The TUNEL assay showed levels of apoptosis consistent with tumor inhibition. These results indicate that BJO could

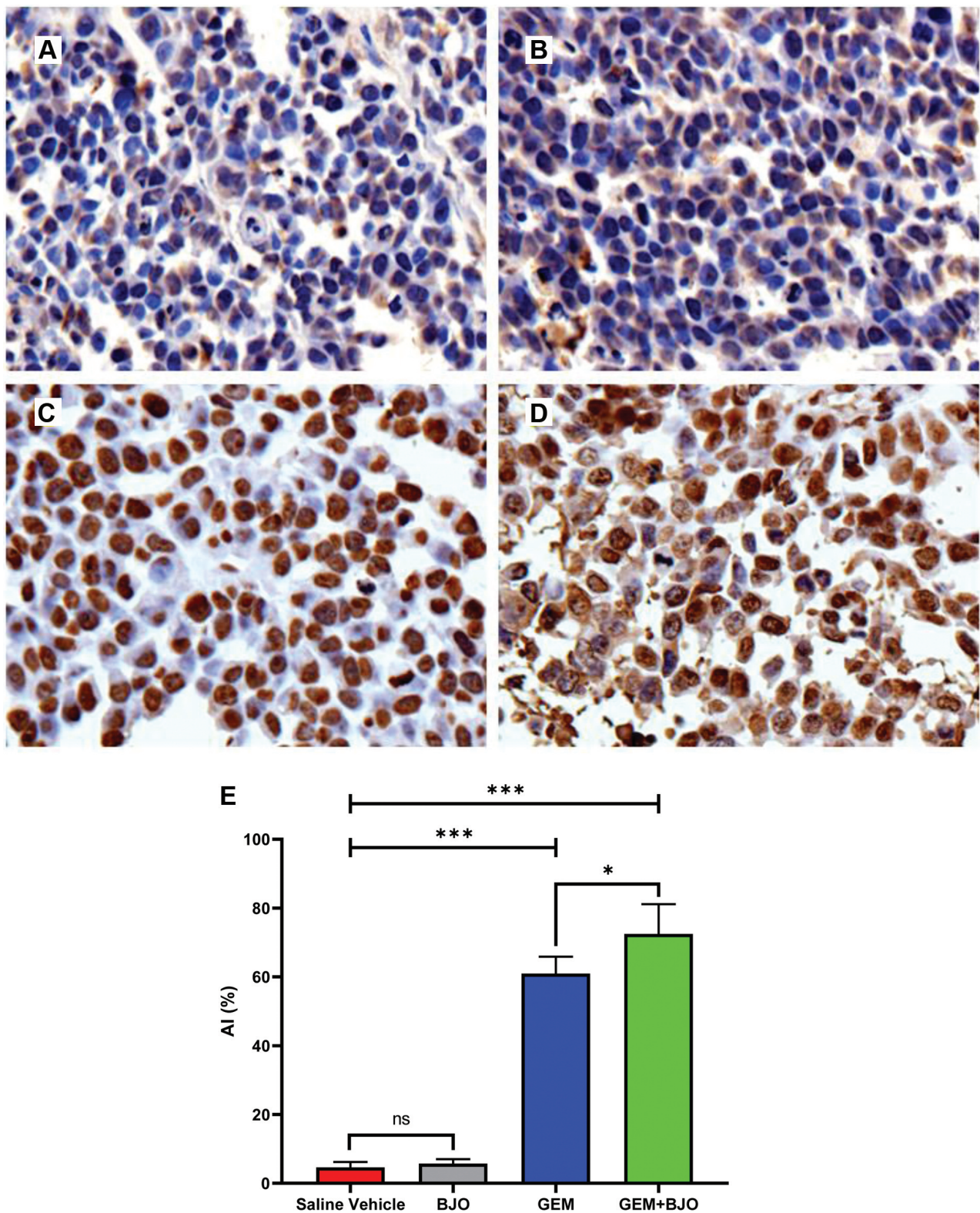


Figure 7. *Brucea javanica* oil (BJO) combined with gemcitabine (GEM) enhanced apoptosis compared to GEM monotherapy in vivo. (A-D) Representative TUNEL images for cellular apoptosis in each group (200× magnification). A: Saline vehicle; B: BJO; C: GEM; D: BJO+GEM. (E) Apoptosis Index (AI) in each group. Data are represented as Mean±SD and analyzed by one-way ANOVA. * $p < 0.05$ (GEM compared to GEM+BJO). *** $p < 0.001$ (GEM compared to Vehicle, GEM+BJO compared to Vehicle).

synergistically enhance GEM monotherapy on pancreatic cancer growth. In the survival evaluation groups, BJO significantly prolonged survival in the pancreatic cancer PDOX model. The molecular mechanisms of BJO efficacy may be related to the activation of mitochondrial pathways to induce apoptosis (25), its effect on autophagy via the PI3K/Akt/mTOR pathway (4), its action on the cell cycle (35), reversing drug resistance (36) or inducing cell differentiation (37). All these mechanisms will be evaluated in the future. We also found that mice had obvious improvements in their physical condition in all BJO treated groups, which may be related to the anti-inflammatory effects of BJO (28).

In conclusion, we demonstrated the power of PDOX mouse model for verifying the efficacy and the potential of BJO for synergistic treatment with first-line chemotherapy for pancreatic cancer. However, because of the extremely complicated components in BJO, which component plays a major role is not clear. In future studies, more experiments need to be performed on the intrinsic molecular mechanisms, including signaling transduction pathways and gene expression. Our laboratory has previously shown that orthotopic models are very appropriate for evaluating TCM (38-41).

Conflicts of Interest

None of the Authors declare any conflicts of interest in this study.

Authors' Contributions

HY and JH designed the study, HY, ZT, LS performed the experiments, YS analyzed the data, HY drafted the manuscript, RMH revised the manuscript, JH administrated and supervised the study.

Acknowledgements

This research was supported by the Health Commission of Hefei, P.R. China (No. hwk2018zc018) and Medical Expert Studio of Hefei, P.R. China.

References

- Rahib L, Smith BD, Aizenberg R, Rosenzweig AB, Fleshman JM and Matrisian LM: Projecting cancer incidence and deaths to 2030: The unexpected burden of thyroid, liver, and pancreas cancers in the united states. *Cancer Res* 74(11): 2913-2921, 2014. PMID: 24840647. DOI: 10.1158/0008-5472.CAN-14-0155
- Li M, Wang MM, Guo XW, Wu CY, Li DR, Zhang X and Zhang PT: Different survival benefits of chinese medicine for pancreatic cancer: How to choose? *Chin J Integr Med* 24(3): 178-184, 2018. PMID: 29063468. DOI: 10.1007/s11655-017-2971-1
- Dong SH, Liu J, Ge YZ, Dong L, Xu CH, Ding J and Yue JM: Chemical constituents from brucea javanica. *Phytochemistry* 85: 175-184, 2013. PMID: 23009875. DOI: 10.1016/j.phytochem.2012.08.018
- Chen X, Li S, Li D, Li M, Su Z, Lai X, Zhou C, Chen S, Li S, Yang X, Su J and Zhang Y: Ethanol extract of brucea javanica seed inhibit triple-negative breast cancer by restraining autophagy via pi3k/akt/mTOR pathway. *Front Pharmacol* 11: 606, 2020. PMID: 32411003. DOI: 10.3389/fphar.2020.00606
- Yan Z, Zhang B, Huang Y, Qiu H, Chen P and Guo GF: Involvement of autophagy inhibition in brucea javanica oil emulsion-induced colon cancer cell death. *Oncol Lett* 9(3): 1425-1431, 2015. PMID: 25663926. DOI: 10.3892/ol.2015.2875
- Wu JR, Liu SY, Zhu JL, Zhang D and Wang KH: Efficacy of brucea javanica oil emulsion injection combined with the chemotherapy for treating gastric cancer: A systematic review and meta-analysis. *Evid Based Complement Alternat Med* 2018: 6350782, 2018. PMID: 29853964. DOI: 10.1155/2018/6350782
- Zhang Y, Zhang L, Zhang Q, Zhang X, Zhang T and Wang B: Enhanced gastric therapeutic effects of brucea javanica oil and its gastroretentive drug delivery system compared to commercial products in pharmacokinetics study. *Drug Des Devel Ther* 12: 535-544, 2018. PMID: 29559770. DOI: 10.2147/DDDT.S155244
- Lau ST, Lin ZX, Zhao M and Leung PS: Brucea javanica fruit induces cytotoxicity and apoptosis in pancreatic adenocarcinoma cell lines. *Phytother Res* 22(4): 477-486, 2008. PMID: 18386257. DOI: 10.1002/ptr.2344
- Talmadge JE, Singh RK, Fidler IJ and Raz A: Murine models to evaluate novel and conventional therapeutic strategies for cancer. *Am J Pathol* 170(3): 793-804, 2007. PMID: 17322365. DOI: 10.2353/ajpath.2007.060929
- Suetsugu A, Katz M, Fleming J, Truty M, Thomas R, Moriwaki H, Bouvet M, Saji S and Hoffman RM: Multi-color palette of fluorescent proteins for imaging the tumor microenvironment of orthotopic tumorgraft mouse models of clinical pancreatic cancer specimens. *J Cell Biochem* 113(7): 2290-2295, 2012. PMID: 22573550. DOI: 10.1002/jcb.24099
- Suetsugu A, Katz M, Fleming J, Truty M, Thomas R, Saji S, Moriwaki H, Bouvet M and Hoffman RM: Non-invasive fluorescent-protein imaging of orthotopic pancreatic-cancer-patient tumorgraft progression in nude mice. *Anticancer Res* 32(8): 3063-3067, 2012. PMID: 22843874.
- Suetsugu A, Katz M, Fleming J, Truty M, Thomas R, Saji S, Moriwaki H, Bouvet M and Hoffman RM: Imageable fluorescent metastasis resulting in transgenic gfp mice orthotopically implanted with human-patient primary pancreatic cancer specimens. *Anticancer Res* 32(4): 1175-1180, 2012. PMID: 22493347.
- Kawaguchi K, Igarashi K, Miyake K, Lwin TM, Miyake M, Kiyuna T, Hwang HK, Murakami T, Delong JC, Singh SR, Clary B, Bouvet M, Unno M and Hoffman RM: Mek inhibitor trametinib in combination with gemcitabine regresses a patient-derived orthotopic xenograft (pdx) pancreatic cancer nude mouse model. *Tissue Cell* 52: 124-128, 2018. PMID: 29857821. DOI: 10.1016/j.tice.2018.05.003
- Kawaguchi K, Miyake K, Han Q, Li S, Tan Y, Igarashi K, Lwin TM, Higuchi T, Kiyuna T, Miyake M, Oshiro H, Bouvet M, Unno M and Hoffman RM: Targeting altered cancer methionine metabolism with recombinant methioninase (rmetase) overcomes partial gemcitabine-resistance and regresses a patient-derived orthotopic xenograft (pdx) nude mouse model of pancreatic cancer. *Cell Cycle* 17(7): 868-873, 2018. PMID: 29623758. DOI: 10.1080/15384101.2018.1445907

- 15 Choi SI, Jeon AR, Kim MK, Lee YS, Im JE, Koh JW, Han SS, Kong SY, Yoon KA, Koh YH, Lee JH, Lee WJ, Park SJ, Hong EK, Woo SM and Kim YH: Development of patient-derived preclinical platform for metastatic pancreatic cancer: Pdox and a subsequent organoid model system using percutaneous biopsy samples. *Front Oncol* 9: 875, 2019. PMID: 31572675. DOI: 10.3389/fonc.2019.00875
- 16 Amin MB, Greene FL, Edge SB, Compton CC, Gershenwald JE, Brookland RK, Meyer L, Gress DM, Byrd DR and Winchester DP: The eighth edition ajcc cancer staging manual: Continuing to build a bridge from a population-based to a more "personalized" approach to cancer staging. *CA Cancer J Clin* 67(2): 93-99, 2017. PMID: 28094848. DOI: 10.3322/caac.21388
- 17 Yang M, Reynoso J, Bouvet M and Hoffman RM: A transgenic red fluorescent protein-expressing nude mouse for color-coded imaging of the tumor microenvironment. *J Cell Biochem* 106(2): 279-284, 2009. PMID: 19097136. DOI: 10.1002/jcb.21999
- 18 Hiroshima Y, Zhao M, Maawy A, Zhang Y, Katz MH, Fleming JB, Uehara F, Miwa S, Yano S, Momiyama M, Suetsugu A, Chishima T, Tanaka K, Bouvet M, Endo I and Hoffman RM: Efficacy of salmonella typhimurium a1-r versus chemotherapy on a pancreatic cancer patient-derived orthotopic xenograft (pdox). *J Cell Biochem* 115(7): 1254-1261, 2014. PMID: 24435915. DOI: 10.1002/jcb.24769
- 19 An Z, Wang X, Kubota T, Moossa AR and Hoffman RM: A clinical nude mouse metastatic model for highly malignant human pancreatic cancer. *Anticancer Res* 16(2): 627-631, 1996. PMID: 8687107.
- 20 Yano S, Hiroshima Y, Maawy A, Kishimoto H, Suetsugu A, Miwa S, Toneri M, Yamamoto M, Katz MH, Fleming JB, Urata Y, Tazawa H, Kagawa S, Bouvet M, Fujiwara T and Hoffman RM: Color-coding cancer and stromal cells with genetic reporters in a patient-derived orthotopic xenograft (pdox) model of pancreatic cancer enhances fluorescence-guided surgery. *Cancer Gene Ther* 22(7): 344-350, 2015. PMID: 26088297. DOI: 10.1038/cgt.2015.26
- 21 Hoffman RM: Orthotopic metastatic (metamouse) models for discovery and development of novel chemotherapy. *Methods Mol Med* 111: 297-322, 2005. PMID: 15911987. DOI: 10.1385/1-59259-889-7:297
- 22 Zhu G, Zhao M, Han Q, Tan Y, Sun Y, Bouvet M, Clary B, Singh SR, Ye J and Hoffman RM: Temozolomide and pazopanib combined with folfox regressed a primary colorectal cancer in a patient-derived orthotopic xenograft mouse model. *Transl Oncol* 13(3): 100739, 2020. PMID: 32143177. DOI: 10.1016/j.tranon.2019.12.011
- 23 Shu Q, Antalffy B, Su JM, Adesina A, Ou CN, Pietsch T, Blaney SM, Lau CC and Li XN: Valproic acid prolongs survival time of severe combined immunodeficient mice bearing intracerebellar orthotopic medulloblastoma xenografts. *Clin Cancer Res* 12(15): 4687-4694, 2006. PMID: 16899619. DOI: 10.1158/1078-0432.CCR-05-2849
- 24 Zhang H, Qi L, Du Y, Huang LF, Braun FK, Kogiso M, Zhao Y, Li C, Lindsay H, Zhao S, Injac SG, Baxter PA, Su JM, Stephan C, Keller C, Heck KA, Harmanci A, Harmanci AO, Yang J, Klisch TJ, Li XN and Patel AJ: Patient-derived orthotopic xenograft (pdox) mouse models of primary and recurrent meningioma. *Cancers (Basel)* 12(6), 2020. PMID: 32517016. DOI: 10.3390/cancers12061478
- 25 Lau ST, Lin ZX, Liao Y, Zhao M, Cheng CH and Leung PS: Bruceine d induces apoptosis in pancreatic adenocarcinoma cell line panc-1 through the activation of p38-mitogen activated protein kinase. *Cancer Lett* 281(1): 42-52, 2009. PMID: 19286308. DOI: 10.1016/j.canlet.2009.02.017
- 26 Phillipson JD and Darwish FA: Bruceolides from filjian brucea javanica. *Planta Med* 41(3): 209-220, 1981. PMID: 7232552. DOI: 10.1055/s-2007-971706
- 27 Pan P, Yang BX and Ge XL: Brucea javanica seed oil enhances the radiosensitivity of esophageal cancer by inhibiting hypoxia-inducible factor 1alpha, *in vitro* and *in vivo*. *Oncol Lett* 15(3): 3870-3875, 2018. PMID: 29456736. DOI: 10.3892/ol.2018.7779
- 28 Huang YF, Zhou JT, Qu C, Dou YX, Huang QH, Lin ZX, Xian YF, Xie JH, Xie YL, Lai XP and Su ZR: Anti-inflammatory effects of brucea javanica oil emulsion by suppressing nf-kappab activation on dextran sulfate sodium-induced ulcerative colitis in mice. *J Ethnopharmacol* 198: 389-398, 2017. PMID: 28119098. DOI: 10.1016/j.jep.2017.01.042
- 29 Jin W, Han H, Zhou S, Wang Y, Dong T and Zhao C: Therapeutic efficacy of brucea javanica oil emulsion (bjoe) combined with transcatheter hepatic arterial chemoembolization (tace) in patients with primary liver cancer. *Int J Clin Exp Med* 8(10): 18954-18962, 2015. PMID: 26770520.
- 30 Nie YL, Liu KX, Mao XY, Li YL, Li J and Zhang MM: Effect of injection of brucea javanica oil emulsion plus chemoradiotherapy for lung cancer: A review of clinical evidence. *J Evid Based Med* 5(4): 216-225, 2012. PMID: 23557502. DOI: 10.1111/jebm.12001
- 31 Qiu ZH, Zhang WW, Zhang HH and Jiao GH: Brucea javanica oil emulsion improves the effect of radiotherapy on esophageal cancer cells by inhibiting cyclin d1-cdk4/6 axis. *World J Gastroenterol* 25(20): 2463-2472, 2019. PMID: 31171890. DOI: 10.3748/wjg.v25.i20.2463
- 32 Zhu X and Pan P: Effect of brucea javanica oil emulsion on proliferation, migration and autophagy of non-small cell lung cancer a549 cells and the underlying mechanisms. *Zhong Nan Da Xue Xue Bao Yi Xue Ban* 43(11): 1202-1208, 2018. PMID: 30643064. DOI: 10.11817/j.issn.1672-7347.2018.11.006
- 33 Bagheri E, Hajiaghaalipour F, Nyamathulla S and Salehen N: The apoptotic effects of brucea javanica fruit extract against ht29 cells associated with p53 upregulation and inhibition of nf-kappab translocation. *Drug Des Devel Ther* 12: 657-671, 2018. PMID: 29636600. DOI: 10.2147/DDDT.S155115
- 34 Fu XY, Besterman JM, Monosov A and Hoffman RM: Models of human metastatic colon cancer in nude mice orthotopically constructed by using histologically intact patient specimens. *Proc Natl Acad Sci USA* 88(20): 9345-9349, 1991. PMID: 1924398. DOI: 10.1073/pnas.88.20.9345
- 35 Zhang H, Yang JY, Zhou F, Wang LH, Zhang W, Sha S and Wu CF: Seed oil of brucea javanica induces apoptotic death of acute myeloid leukemia cells via both the death receptors and the mitochondrial-related pathways. *Evid Based Complement Alternat Med* 2011: 965016, 2011. PMID: 21760826. DOI: 10.1155/2011/965016
- 36 Ren D, Villeneuve NF, Jiang T, Wu T, Lau A, Toppin HA and Zhang DD: Brusatol enhances the efficacy of chemotherapy by inhibiting the nrf2-mediated defense mechanism. *Proc Natl Acad Sci USA* 108(4): 1433-1438, 2011. PMID: 21205897. DOI: 10.1073/pnas.1014275108
- 37 Cuendet M, Gills JJ and Pezzuto JM: Brusatol-induced hl-60 cell differentiation involves nf-kappab activation. *Cancer Lett* 206(1): 43-50, 2004. PMID: 15019158. DOI: 10.1016/j.canlet.2003.11.011

- 38 Hu M, Zhao M, An C, Yang M, Li Q, Zhang Y, Suetsugu A, Tome Y, Yano S, Fu Y, Hoffman RM and Hu K: Real-time imaging of apoptosis induction of human breast cancer cells by the traditional chinese medicinal herb tubeimu. *Anticancer Res* 32(7): 2509-2514, 2012. PMID: 22753707.
- 39 Zang W, Bian H, Huang X, Yin G, Zhang C, Han LI, Hao P, Ding S, Sun YU, Yang Z, Hoffman RM and Tang D: Traditional chinese medicine (tcm) astragalus membranaceus and curcuma wenyujin promote vascular normalization in tumor-derived endothelial cells of human hepatocellular carcinoma. *Anticancer Res* 39(6): 2739-2747, 2019. PMID: 31177109. DOI: 10.21873/anticancer.13400
- 40 Yin G, Tang D, Dai J, Liu M, Wu M, Sun YU, Yang Z, Hoffman RM, Li L, Zhang S and Guo X: Combination efficacy of astragalus membranaceus and curcuma wenyujin at different stages of tumor progression in an imageable orthotopic nude mouse model of metastatic human ovarian cancer expressing red fluorescent protein. *Anticancer Res* 35(6): 3193-3207, 2015. PMID: 26026079.
- 41 Dai X, Liu D, Liu M, Zhang X, Wang W, Jin F, Qian Y, Wang X, Zhao J, Wu Y, Xiong F, Chang NA, Sun YU, Yang Z, Hoffman RM and Liu Y: Anti-metastatic efficacy of traditional chinese medicine (tcm) ginsenoside conjugated to a vefgr-3 antibody on human gastric cancer in an orthotopic mouse model. *Anticancer Res* 37(3): 979-986, 2017. PMID: 28314255. DOI: 10.21873/anticancer.11407

Received July 8, 2020

Revised July 27, 2020

Accepted July 28, 2020